Front. Earth Sci. 2015, 9(1): 13–25
DOI 10.1007/s11707-014-0464-5

RESEARCH ARTICLE

Paleoaltimetry proxies based on bacterial branched tetraether membrane lipids in soils

Huan YANG[1], Wenjie XIAO[1], Chengling JIA[2], Shucheng XIE (✉)[1]

1 State Key Laboratory of Biogeology and Environmental Geology, China University of Geosciences, Wuhan 430074, China
2 State Key Laboratory of Marine Geology, Tongji University, Shanghai 200092, China

Abstract The MBT/CBT (Methylation Index of Branched Tetraethers/Cyclisation ratio of Branched Tetraether) proxy, a terrestrial paleothermometer based on bacterial branched glycerol dialkyl glycerol tetraethers (bGDGTs), was employed to indicate altimetry; however, the mechanistic control on this proxy is still ambiguous. Here, we investigated the bGDGTs' distribution and associated environmental factors along an altitude transect of Mt. Shennongjia in China in order to determine the applicability of bGDGT-based proxies to altimetry reconstruction. The MBT index exhibits only a weak correlation with estimated mean annual air temperature (MAT_e, estimated according to the meteorological record and lapse rate) or altitude. Likewise, MBT shows weak or no relationship with temperature or altitude at four other mountains (Mts. Meghalaya, Jianfengling, Gongga, and Rungwe). It is notable that mean annual air temperature (MAT) or altitude estimated by the MBT/CBT proxy largely relies on CBT, rather than on MBT, which was generally acknowledged. The poor relationship between MBT and MAT_e for Mt. Shennongjia can be ascribed to the insensitive response of bGDGT-I to temperature. Our data from this mountain imply that care should be taken if the MBT/CBT proxy is employed as an indication of paleoaltimetry. We propose that the fractional abundance of bGDGTs may be a better paleoaltimeter than the MBT/CBT proxy, because specific bGDGT subsets that might show the most sensitive response to temperature can be preferentially selected using a statistical method and used to establish local calibration. This local calibration was applied to Mt. Shennongjia and apparently improves the accuracy of temperature and altimetry reconstruction. The differential response of bGDGTs to temperature among mountains suggests that local calibrations are needed to better constrain the altimetry.

Received January 20, 2014; accepted March 20, 2014

E-mail: xiecug@163.com

Keywords branched glycerol dialkyl glycerol tetraethers, soil pH, paleoaltimetry, temperatures

1 Introduction

The evolution of topography provides information about the interaction among earth crust, upper mantle, and surface erosion during mountain and plateau formation. The uplift of plateau can change the atmospheric circulation and in turn impact the onset or intensification of the monsoon system (Ruddiman and Kutzbach, 1989). A combination of different approaches is generally required to better constrain the paleoaltimetry. Development of new paleoaltimetry proxies that can be used widely in diverse sample types is therefore of crucial importance in understanding the relation between the landscape and paleoclimate change. Recent paleoaltimetry reconstruction largely depends on the change in temperature and isotopic composition of precipitation due to the 'altitude effect' (Rowley and Garzione, 2007; Polissar et al., 2009). Numerous proxies for terrestrial paleotemperature and paleohydrology have been proposed or used as paleoaltimeters, including clumped ^{13}C-^{18}O isotopes (Ghosh et al., 2006), the hydrogen isotopes of kaolinite or muscovite (Mulch et al., 2004, 2006), *n*-alkanes derived from the epicuticular wax of plants (Jia et al., 2008; Luo et al., 2011), and the tetraether lipid-based MBT/CBT (Methylation Index of Branched Tetraethers/Cyclisation ratio of Branched Tetraether) proxy and TEX_{86} (Sinninghe Damsté et al., 2008; Peterse et al., 2009; Yang et al., 2010; Ernst et al., 2013; Liu et al., 2013). However, each proxy has potential weaknesses and the accurate estimation of paleoaltimetry based on these proxies principally relies on surveys of modern environments for establishing the relationship of proxies with modern climatic parameters (or altitude). This necessitates a comprehensive understanding of the inherent mechanisms of these paleoalti-

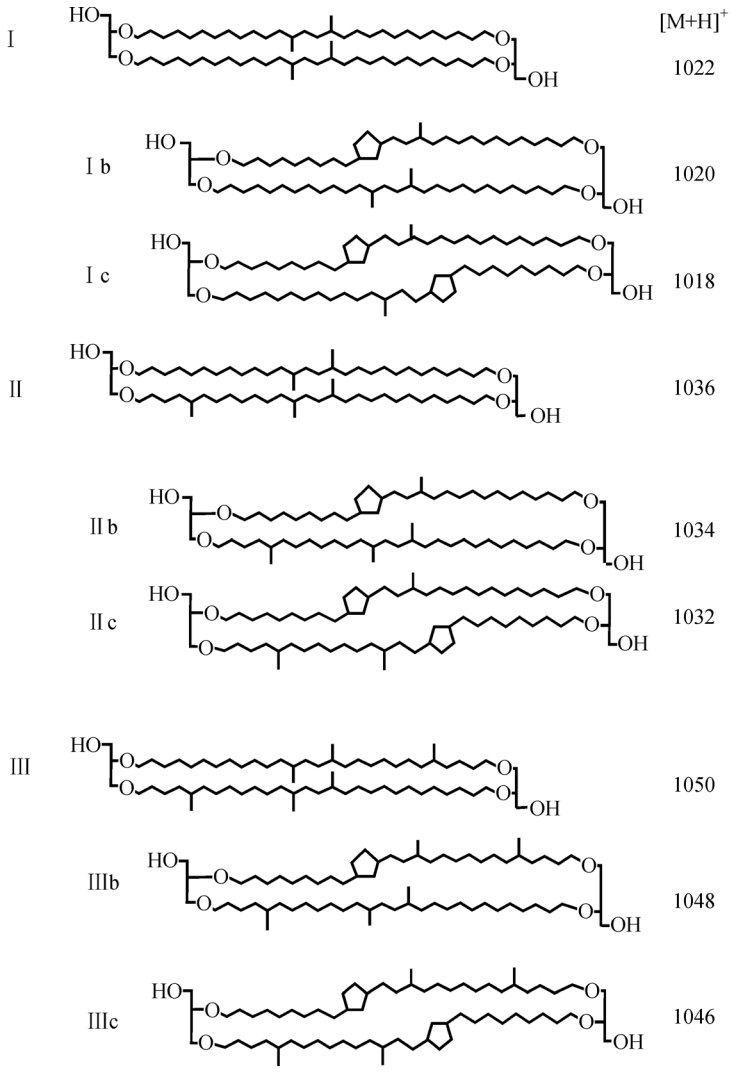

Fig. 1 Structures of branched GDGTs and their mass to charge ratios (*m/z*).

metry proxies in more modern altitude transects.

The MBT/CBT proxy (or MBT'/CBT) derived from the bacterial glycerol dialkyl glycerol tetraethers (bGDGTs) has been employed to indicate terrestrial paleotemperature and subsequently paleoaltimetry (Weijers et al., 2007; Hren et al., 2010; Peterse et al., 2012; Yang et al., 2014). The bGDGTs, a suite of membrane lipids from as yet unknown bacteria with a heterotrophic lifestyle (Weijers et al., 2010), are comprised of two glycerol backbones bound to two alkyl chains, each of which contains 1 to 3 methyl moieties and 0 to 1 cyclopentyl moieties (Sinninghe Damsté et al., 2000; Weijers et al., 2007) (Fig. 1). These lipids are ubiquitous in terrestrial environments and relatively abundant in peats, organic-rich soils, and lacustrine sediments (Weijers et al., 2006, 2011; Tierney et al., 2010; Yang et al., 2011, 2014); this allows for the application of the MBT/CBT proxy as a paleoaltimeter to numerous kinds of sample types. The MBT, which reflects the methylation degree of bGDGTs, has been found to have a linear correlation with temperature and to a lesser extent to soil pH. CBT, which represents the cyclization degree of bGDGTs, is only strongly related to soil pH (Weijers et al., 2007; Peterse et al., 2012; Yang et al., 2014). The MBT and CBT indices were combined to form an MBT/CBT proxy, by which mean annual air temperature (MAT) can be reasonably reconstructed. The MBT proxy appears to be also influenced by other confounding factors, such as soil humidity, etc. (Loomis et al., 2011), which could complicate the use of the MBT/CBT proxy in paleoaltimetry reconstruction. Therefore, further validation of the relationship of the MBT/CBT index with temperature along more altitude transects is needed.

For this study we collected surface soils along an altitudinal transect at Mt. Shennongjia in Central China and tested the applicability of bGDGT-based proxies to altimetry reconstruction. We also compiled the previously published data of bGDGTs along the altitude transects of seven other mountains, summarized the relationship

between the MBT/CBT index and altitude, and examined the complexity of the MBT/CBT proxy being used as a paleoaltimeter.

2 Materials and methods

2.1 Soil sampling

Mt. Shennongjia is a natural reserve in central China, ca. 400 km to the west of Wuhan, the capital city of the Hubei Province (Fig. 2). The summit of this mountain has an elevation of 3,106 m above sea level (a.s.l.) while the lowest elevation is 398 m. The mountain has a clear vegetation and climate zonation as a result of the altitude effect. The alpine meadow and coniferous trees dominate at high altitudes > 2,500 m whereas deciduous broad-leaved trees dominate below that altitude. Mt. Shennongjia is subjected to the East Asian summer monsoon and winter monsoon with temperature and rainfall maximizing in summer. The MAT for 1971–2000, monitored at the Shennongjia meteorological station (GPS position: 31.75°N, 110.67°E; altitude: 937.2 m), is 12.1°C. Mean annual precipitation (MAP) shows the opposite trend with increased elevation, exhibiting a cold/humid climate and relatively warm/dry climate at the peak and foot, respectively.

Twenty-eight surface soils in A horizon with depth < 10 cm were collected along an altitude transect of Mt. Shennongjia between 316 m and 2,907 m a.s.l. at ca. 200–300 m intervals after removing the litter layer. Soils from three to four spots at a given site were combined and homogenized to form a sample, and 2 to 3 samples were collected at each altitude. The altitude, latitude, and longitude at each sampling site were measured using a portable GPS. Samples were transported to the laboratory soon after collection and stored at –20°C in a refrigerator.

2.2 Environmental variables

During soil sampling, 3 to 6 air and soil temperatures were measured in situ using a digital thermometer, yielding a total of 50 sets of data along the altitude transect. Soils encapsulated in aluminum foil were freeze dried and the weight of soil was determined using a digital balance before and after drying. The soil water content (SWC) was calculated based on Eq. (1) as below.

$$\mathrm{SWC} = (W_{\mathrm{ws}} - W_{\mathrm{ds}})/W_{\mathrm{ws}}, \quad (1)$$

where W_{ws} and W_{ds} denote the weight of wet and dry soil, respectively.

The transfer function between altitude and MAT developed by Zhu et al. (2008) provided the estimation of MAT at a given altitude of Mt. Shennongjia. The estimated MAT ($\mathrm{MAT_e}$) for the sampling sites ranged from 1.0°C to 16.7°C with a lapse rate of 0.61°C/(100 m).

Soil pH was determined according to the method described by Yang et al. (2012). The homogenized soil powder was mixed with ultrapure water in a ratio of 1:2.5 (g: mL). The mixture was stirred by a vortex and allowed to stand for 30 min for phase separation. The pH of the supernatant was measured with a pH meter (±0.1 pH unit)

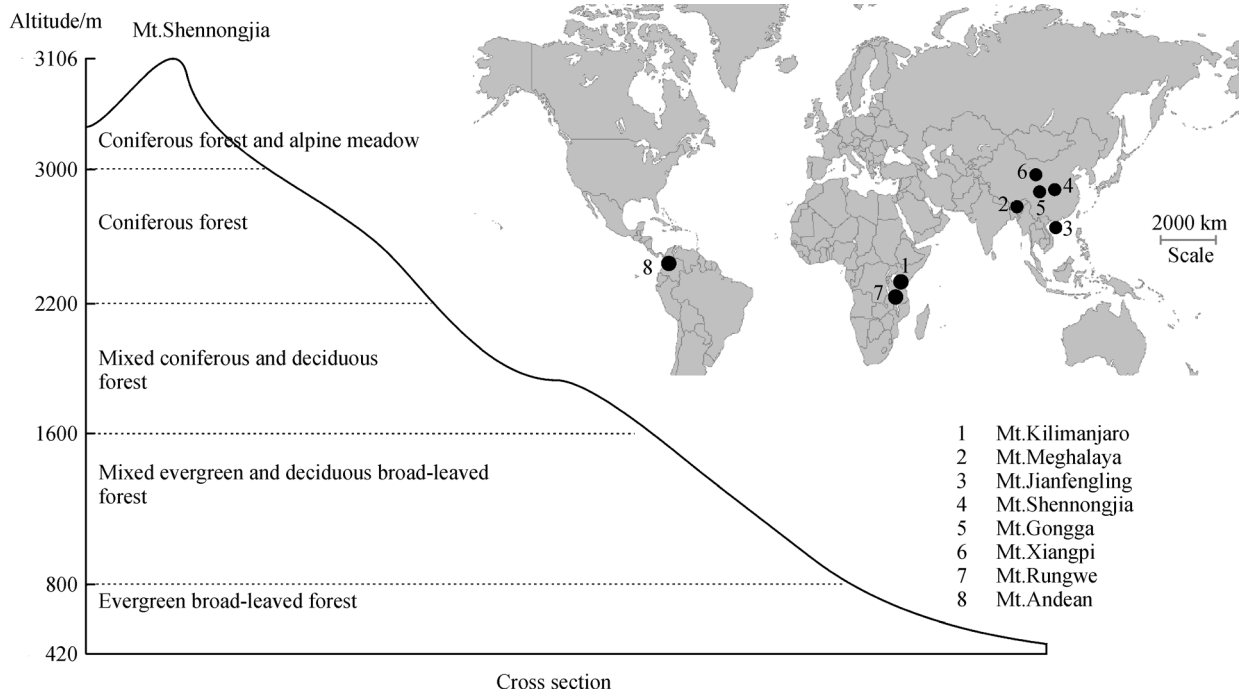

Fig. 2 The altitudinal zonation of vegetation for Mt. Shennongjia and the locations of mountains discussed in the study on the world map.

three times, and the final pH value for each soil was the average of the three measurements.

2.3 Lipid extraction, fractionation and instrumentation

An aliquot of soil samples (6–8 g) was ultrasonically extracted with dichloromethane (DCM) and methanol (MeOH) (9:1, v/v) in a water bath. The volume of the resulting total lipid extract (TLE) was condensed to 2–3 mL by a rotary evaporator under reduced pressure. The TLE was further separated into alkanes and polar lipids on a silica gel flash column with *n*-hexane and MeOH as eluents, respectively. Half of the polar fraction was filtrated through 0.45 μm PTFE syringe filters and dried under nitrogen gas.

The dried polar fraction was re-dissolved in 290 μL of *n*-hexane/isopropanol (99:1, v/v) and spiked with 10 μL of synthesized internal standard C_{46} GDGT (Huguet et al., 2006). GDGTs were analyzed by an Agilent 1200 series liquid chromatography (LC) tandem mass spectrometer (MS^2), equipped with autosampler and ChemStation manager software. The injection volume varied from 10 to 30 μL, and GDGT compounds were separated with an Alltech Prevail Cyano column (150 mm × 2.1 mm, 3 μm). The flow rate was 0.2 mL/min, and the eluent gradient varied according to the following process: it was initially 90% A/10% B, held isocratically for 5 min, followed by 82% A/18% B from 5 to 45 min, then held at 100% B for 10 min to wash the column, and finally back to 90% A/10% B in order to re-equilibrate the column, where A = *n*-hexane and B = *n*-hexane/isopropanol (9:1, v/v). GDGTs were ionized in an atmospheric pressure chemical ionization (APCI) chamber with single ion monitoring (SIM), monitoring *m/z* 1302.3, 1300.3, 1298.3, 1296.3, 1292.3, 1050, 1048, 1046, 1036, 1034, 1032, 1022, 1020, and 1018. Compounds were quantified by a peak area integration of $[M + H]^+$ (protonated molecular ion) in the extracted ion chromatogram. Because the relative response factor between crenarchaeol and the internal standard (C_{46} GDGT) was not determined, the final quantification results can only be considered semi-quantitative. The data reported are thus not absolute concentrations, but allowed comparison between samples. All samples were run in duplicate and the average of two measurements was reported as final data. Proxies including MBT and CBT were calculated according to following formula.

$$\mathrm{MBT} = (\mathrm{I} + \mathrm{Ib} + \mathrm{Ic})/(\mathrm{I} + \mathrm{Ib} + \mathrm{Ic} + \mathrm{II} + \mathrm{IIb} + \mathrm{IIc} + \mathrm{III} + \mathrm{IIIb} + \mathrm{IIIc}), \quad (2)$$

$$\mathrm{CBT} = -\log\Big((\mathrm{Ib} + \mathrm{IIb})/(\mathrm{I} + \mathrm{II})\Big). \quad (3)$$

The fractional abundance of each bGDGT was calculated based on Eq. (4):

$$f(i) = i/(\mathrm{I} + \mathrm{Ib} + \mathrm{Ic} + \mathrm{II} + \mathrm{IIb} + \mathrm{IIc} + \mathrm{III} + \mathrm{IIIb} + \mathrm{IIIc}). \quad (4)$$

2.4 Data processing

Multiple and binary linear regression analyses were performed using SPSS version 19 software. The CANOCO version 4.5 software was employed in order to ascertain the relationship between environmental variables and fractional abundances of bGDGTs (ter Braak and Smilauer, 2002). First, we used detrended correspondence analysis (DCA) in order to determine which method (linear or non-linear) fit best with our bGDGT dataset according to the length of the gradient (ter Braak, 1988; ter Braak and Prentice, 1988). The result showed that a linear model suits our dataset because the gradient length is < 3. Redundancy analysis (RDA), a 'constrained' version of Principal Component Analysis (PCA), was also performed on our dataset so that the environmental variable that can best explain the variations in the fractional abundance of each bGDGT was directly visualized (ter Braak and Smilauer, 2002).

3 Results and discussion

3.1 Environmental variables along the altitude transect

The air and soil temperatures measured in situ vary in large amplitudes along the altitudinal transect of Mt. Shennongjia (Table 1). The in situ air temperature might be more affected by tree shades, winds, and vegetation cover,

Table 1 Sampling information for soils collected along an altitudinal transect of Mt. Shennongjia in Hubei, China.

Sample No.	Air T/°C	Soil T/m	Alt./m [a)]	Latitude (N)	Longitude (E)	Depth/cm	MAT_e/°C [b)]	SWC	pH
3-5	13.2	9.2	2907	31°27.093′	110°16.150′	6	1.0	0.37	5.30
3-4	15.1	9.6	2882	31°27.083′	110°16.116′	10	1.1	0.33	5.98
3-3	13.8	10.8	2861	31°27.069′	110°16.102′	7	1.2	0.38	5.84
3-2	11.2	10.5	2847	31°27.053′	110°16.052′	7	1.3	0.38	4.95
3-1	14.4	10.6	2840	31°27.045′	110°16.036′	7	1.4	0.36	5.94
3-6	16.9	11.7	2824	31°26.591′	110°16.362′	10	1.5	–	5.82

(*Continued*)

Sample No.	Air T/°C	Soil T/m	Alt./m [a]	Latitude (N)	Longitude (E)	Depth/cm	MAT_e/°C [b]	SWC	pH
4-1	20.2	12.9	2632	31°26.633′	110°17.414′	9	2.6	0.45	5.03
4-2	18.1	10.6	2632	31°26.628′	110°17.414′	10	2.6	0.33	4.74
4-3	18.1	10.6	2632	31°26.628′	110°17.414′	10	2.6	0.48	5.00
5-1	21.5	13.1	2386	31°27.878′	110°17.285′	10	4.1	0.39	5.81
5-2	21.5	12.5	2386	31°27.878′	110°17.285′	10	4.1	0.32	5.46
5-3	21.5	12.1	2386	31°27.878′	110°17.285′	8	4.1	0.41	5.70
5-4	21.5	11.9	2386	31°27.878′	110°17.285′	10	4.1	0.35	5.47
6-1	21.0	13.5	2187	31°28.578′	110°18.108′	8	5.3	–	7.50
6-2	21.0	11.1	2187	31°28.578′	110°18.108′	9	5.3	0.36	
6-3	21.0	10.9	2187	31°28.578′	110°18.108′	8	5.3	0.37	6.36
6-4	21.0	11.3	2187	31°28.578′	110°18.108′	7	5.3	0.36	6.40
7-1	20.3	12.0	1986	31°29.955′	110°19.181′	7	6.4	0.28	6.78
7-2	20.3	11.9	1986	31°29.955′	110°19.181′	10	6.4	0.30	6.59
7-4	20.3	18.1	1986	31°29.955′	110°19.181′	8	6.4	–	6.76
8-1	20.3	17.2	1790	31°29.757	110°21.431′	8	7.6	0.23	6.47
8-2	20.3	17.1	1790	31°29.757	110°21.431′	9	7.6	0.24	6.91
1-1	23.5	20.2	1770	31°32.654′	109°59.706′	–	7.7	0.26	4.12
1-2	23.5	20.2	1770	31°32.654′	109°59.706′	–	7.7	0.32	4.49
1-3	22.3	18.1	1770	31°32.654′	109°59.706′	–	7.7	0.46	
8-4	20.3	19.1	1770	31°29.757	110°21.431′	10	7.7	0.16	7.98
2-1	21.2	14.3	1763	31°28.914′	109°59.012′	8	7.8	0.42	5.13
8-3	20.3	16.1	1750	31°29.757	110°21.431′	10	7.9	0.23	7.71
9-4	19.8	17.9	1594	31°29.977′	110°22.061′	8	8.8	0.28	5.83
9-2	19.8	21.0	1592	31°29.977′	110°22.061′	6	8.8	0.22	5.33
9-1	19.8	18.4	1588	31°29.977′	110°22.061′	7	8.8	0.28	6.06
10-1	20.1	17.2	1333	31°28.525′	110°23.070′	2	10.4	–	7.63
10-2	20.1	17.7	1329	31°28.525′	110°23.070′	8	10.4	0.23	7.06
10-3	20.1	20.4	1322	31°28.525′	110°23.070′	10	10.4	0.24	6.84
10-4	20.1	20.6	1322	31°28.525′	110°23.070′	10	10.4	0.27	6.26
11-1	20.0	19.4	856	31°23.781′	110°28.701′	7	13.4	0.22	5.03
11-2	20.0	19.0	852	31°23.816′	110°28.672′	6	13.4	0.23	4.87
11-4	19.2	17.5	832	31°23.759′	110°28.878′	7	13.5	0.18	6.63
11-3	20.3	17.8	831	31°23.765′	110°28.880′	7	13.5	0.20	6.83
12-1	24.6	20.2	603	31°20.222′	110°33.678′	2	15.0	0.12	7.93
12-2	24.6	21.0	592	31°20.192′	110°33.717′	2	15.0	0.08	8.01
12-3	24.6	19.0	586	31°20.183′	110°33.723′	8	15.1	0.20	6.44
12-4	24.6	18.9	586	31°20.183′	110°33.723′	6	15.1	0.22	6.84
12-5	24.6	19.3	586	31°20.183′	110°33.723′	6	15.1	0.24	7.23
13-3	25.4	21.8	317	31°20.668′	110°38.210′	6	16.7	0.18	6.94
13-2	25.1	23.2	316	31°20.662′	110°38.206′	6	16.7	0.15	6.86
13-4	25.4	22.0	316	31°20.668′	110°38.213′	2	16.7	0.16	5.91
13-1	25.1	20.4	315	31°20.681′	110°38.194′	2	16.7	0.13	7.56

Note: a) altitude; b) MAT_e was calculated based on the transfer function reported by Zhu et al. (2008): MAT = 61.657–1.375×Latitude–0.006×Altitude.

yielding a reasonably lower correlation (R^2 = 0.55, $p < 0.05$) with altitude than with in situ soil temperature (R^2 = 0.76, $p < 0.05$). However, the correlations are still significant between both in situ air and soil temperature and altitude, suggesting a clear temperature transect at the sampling sites along the altitudes. The estimated MAT (MAT_e) for the sampling sites based on the transfer function of Zhu et al. (2008) ranges from 1.0°C to 16.7°C with a lapse rate of 0.61°C/(100 m), indicating that the climate for this altitude transect spans from subtropical to temperate zones. The SWC also has a significant positive linear correlation with altitude (R^2 = 0.72, $p < 0.001$), reflecting a trend opposite to that of MAT_e and likely increased rainfall with altitudes. Therefore, a cold and humid climate dominates at the top, whereas a relatively warmer and drier climate is found at the foot of Mt. Shennongjia, which is different from the climate pattern on the Eurasian continent, where an increasingly cold and dry climate gradually prevails polewards. The soil pH varies from 4.12 to 7.98, suggesting a dominance of acid soils at Mt. Shennongjia. Soil pH has a weak correlation with altitude or MAT_e (R^2 = 0.21), but exhibits a significant negative correlation with SWC (R^2 = 0.42, $p < 0.01$). The soil pH at low altitudes is overall greater than that at high altitudes, indicating that SWC and in turn precipitation may play a role in the regulation of soil pH at Mt. Shennongjia; this is consistent with the observation by Yang et al. (2014) that soil pH increases dramatically with decreased precipitation from south to north China.

3.2 bGDGTs distribution along the altitude transect of Mt. Shennongjia

A characteristic distribution of GDGTs for acid and humid soils (cf., Weijers et al., 2007; Yang et al., 2014), i.e., the dominance of bGDGTs over iGDGTs in abundance, can be observed in all soils along the altitude transect (Fig. 3). In soils from low altitude, bGDGT-I is generally the most abundant, followed by II. The bGDGT-Ib and IIb, which dominate in cyclic bGDGTs, are usually more abundant than acyclic bGDGT-III in these soils. The bGDGTs with two cyclopentyl rings, IIc and IIIc, are very low in abundance and even below the detection limit. The proportion of bGDGT-II increases with altitude, resulting in a dominance of II in soils from high altitudes.

The significant change in the distribution of bGDGTs with altitude can be reflected by MBT and CBT indices. The MBT value varies from 0.21 to 0.75 and the CBT value varies from 0.14 to 1.43 for the altitude transect; the former exhibits an overall declining trend with altitude (Table 2). However, the lowest MBT values (0.21 and 0.27) do not occur at the highest altitude where the MAT_e is the lowest. Instead, they are found in alkaline and neutral soils; this is consistent with the generally low MBT values in alkaline soils from northern China and the western USA (Dirghangi et al., 2013; Yang et al., 2014). The occurrence of low MBT values in alkaline soils with abundant rainfall (~1,500 mm per year) suggests that high soil pH, rather than low precipitation, is the key factor that results in very

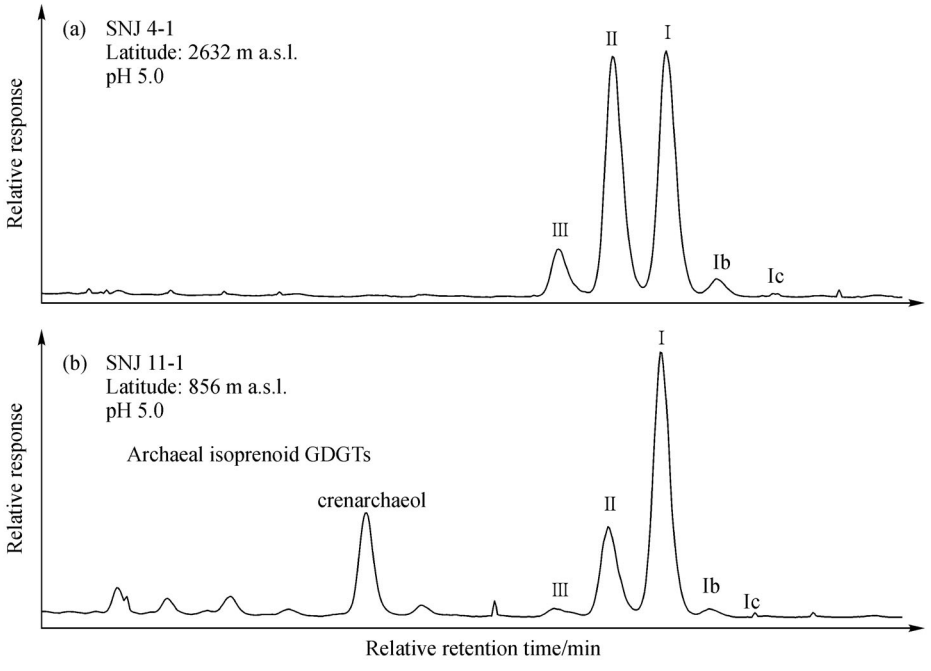

Fig. 3 HPLC-APCI/MS base peak chromatograms showing the distribution of bGDGTs at (a) high and (b) low latitudes of Mt. Shennongjia. The increased abundance of bGDGT-II and III at high altitude is likely the adaptation of bacteria to decreased temperature.

Table 2 The bGDGT-based parameters for selected 28 soil samples from an altitudinal transect of Mt. Shennongjia. The bGDGTs data presented is the fractional abundance of each bGDGT in all bGDGTs.

Sample No.	MBT	CBT	I	II	III	Ib	Ic	IIb	IIc	IIIb	IIIc
3-5	0.39	1.30	0.36	0.46	0.13	0.03	0.01	0.01	0.00	0.00	0.00
3-2	0.37	1.29	0.34	0.46	0.15	0.03	0.00	0.02	0.00	0.00	0.00
3-1	0.42	1.20	0.38	0.44	0.11	0.04	0.00	0.02	0.00	0.00	0.00
4-1	0.47	1.23	0.43	0.43	0.08	0.04	0.00	0.01	0.00	0.00	0.00
4-2	0.43	1.19	0.39	0.42	0.13	0.03	0.00	0.02	0.00	0.00	0.00
5-1	0.39	1.07	0.34	0.44	0.13	0.04	0.01	0.03	0.00	0.00	0.00
5-2	0.39	1.08	0.34	0.45	0.13	0.04	0.01	0.03	0.00	0.00	0.00
5-3	0.36	1.04	0.31	0.46	0.15	0.04	0.01	0.03	0.00	0.00	0.00
5-4	0.42	0.88	0.34	0.43	0.12	0.07	0.01	0.03	0.00	0.00	0.00
6-1	0.30	0.52	0.22	0.36	0.19	0.06	0.02	0.11	0.01	0.01	0.01
6-2	0.36	0.53	0.24	0.39	0.13	0.09	0.03	0.10	0.01	0.01	0.00
6-4	0.39	0.62	0.27	0.40	0.12	0.09	0.04	0.07	0.01	0.00	0.00
7-2	0.38	0.75	0.27	0.40	0.11	0.03	0.03	0.09	0.01	0.00	0.00
7-4	0.41	0.64	0.26	0.37	0.09	0.05	0.05	0.10	0.01	0.00	0.00
1-1	0.62	0.99	0.54	0.32	0.04	0.07	0.01	0.02	0.00	0.00	0.00
1-2	0.62	0.99	0.54	0.32	0.03	0.07	0.01	0.02	0.00	0.00	0.00
8-4	0.21	0.14	0.11	0.30	0.22	0.09	0.01	0.21	0.01	0.03	0.00
2-1	0.51	1.28	0.48	0.40	0.07	0.03	0.00	0.01	0.00	0.00	0.00
9-1	0.59	0.64	0.44	0.31	0.05	0.12	0.02	0.05	0.00	0.00	0.00
10-2	0.27	0.24	0.16	0.34	0.17	0.10	0.01	0.18	0.01	0.02	0.00
10-3	0.37	0.36	0.25	0.34	0.12	0.11	0.02	0.14	0.01	0.01	0.00
11-1	0.72	1.43	0.69	0.24	0.03	0.03	0.01	0.01	0.00	0.00	0.00
11-4	0.54	0.42	0.34	0.29	0.06	0.15	0.05	0.09	0.01	0.01	0.00
11-3	0.50	0.32	0.29	0.30	0.07	0.17	0.04	0.12	0.01	0.01	0.00
12-3	0.63	0.72	0.50	0.28	0.04	0.10	0.03	0.04	0.00	0.00	0.00
12-5	0.50	0.33	0.30	0.28	0.08	0.15	0.04	0.12	0.01	0.01	0.00
13-2	0.66	0.44	0.44	0.23	0.04	0.18	0.05	0.06	0.01	0.00	0.00
13-4	0.75	0.86	0.63	0.20	0.02	0.09	0.03	0.02	0.00	0.00	0.00

low MBT values in soils from Northern China (cf., Yang et al., 2014). The SWC is unlikely to directly impact the functioning and lipid distribution of cell membranes by the addition of water because the bacteria can only thrive in an aqueous solution. The MBT value for soils from high altitudes ($>2{,}500$ m a.s.l.) ranges from 0.37 to 0.47, apparently larger than those two values for alkaline and neutral soils at Mt. Shennongjia. As stated previously by Yang et al. (2014), these MBT values from high altitudes are systematically larger than those for alkaline soils from the cold and dry Chinese loess plateau, implying that besides temperature, soil pH is another important factor that determines MBT values in soils.

3.3 The relationship between bGDGT-based proxies and environmental variables

A RDA plot and correlation matrix were used to determine the influence of environmental variables on the distribution of bGDGTs, and indicate that MBT and CBT indices are moderately to highly correlated with MAT_e and soil pH (Fig. 4). The first two axes of RDA cumulatively account for 47.8% of the variance in the bGDGT distribution. Axis 1, primarily reflecting the gradients in MAT_e (or altitude) and soil pH, can account for 38.7% of the variance, but axis 2 only explains 9.1% of the bGDGT distribution.

Unlike the global dataset (Weijers et al., 2007; Peterse et al., 2012) and Chinese dataset (Yang et al., 2014), the MBT only shows a weak correlation with altitude or MAT_e (R^2= 0.38, $p < 0.01$), and exhibits even a weaker correlation with soil pH (R^2= 0.15, $p < 0.05$), yielding the following equation for the former (Fig. 5(a)):

$$\mathrm{MBT} = 0.017 \times \mathrm{MAT_e} + 0.33 \quad (R^2 = 0.38, p<0.01). \tag{5}$$

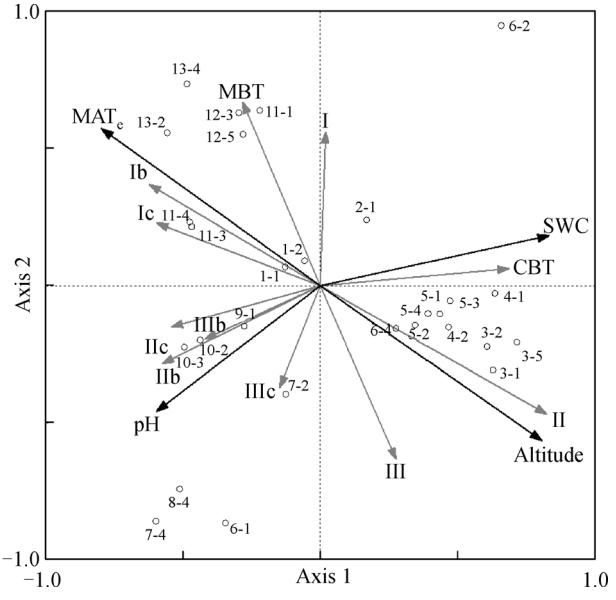

Fig. 4 Redundancy analysis (RDA) triplot showing the relationship between bGDGT-based proxies and environmental variables. I, II, and Ib, etc. represent the fractional abundance of corresponding bGDGTs. Numbers refer to corresponding samples in Table 2.

Although both correlations are very weak, substantial improvement in the coefficient of determination (R^2 from 0.37 to 0.83) can be observed if MAT_e and soil pH are plotted against MBT in a triple linear correlation model:

$$MBT = 0.889 - 0.103 \times pH + 0.025 \times MAT_e \quad (R^2 = 0.83,\ p<0.001). \quad (6)$$

This equation has very similar constant and coefficient to the global calibration proposed by Weijers et al. (2007), who used mainly acid soils as well as a small proportion of alkaline soils. In fact, if two alkaline or neutral soils with uncommonly low MBT values are excluded in the statistics, the determination coefficient for Eq. (5) can be markedly improved (R^2 = 0.54). Hence, the scatter of Eq. (5) may be partly due to the large heterogeneity in soil pH along the altitude transect.

In the RDA plot, the cyclic bGDGTs including Ib, Ic, IIb, and IIc, etc. are closely related to soil pH (Fig. 4), which provides the basis for pH reconstruction using CBT proxy. As expected, the CBT index shows a significant negative correlation with soil pH, suggesting that CBT proxy is a robust proxy for pH in global acid soils. The correlation can be described by the following equation

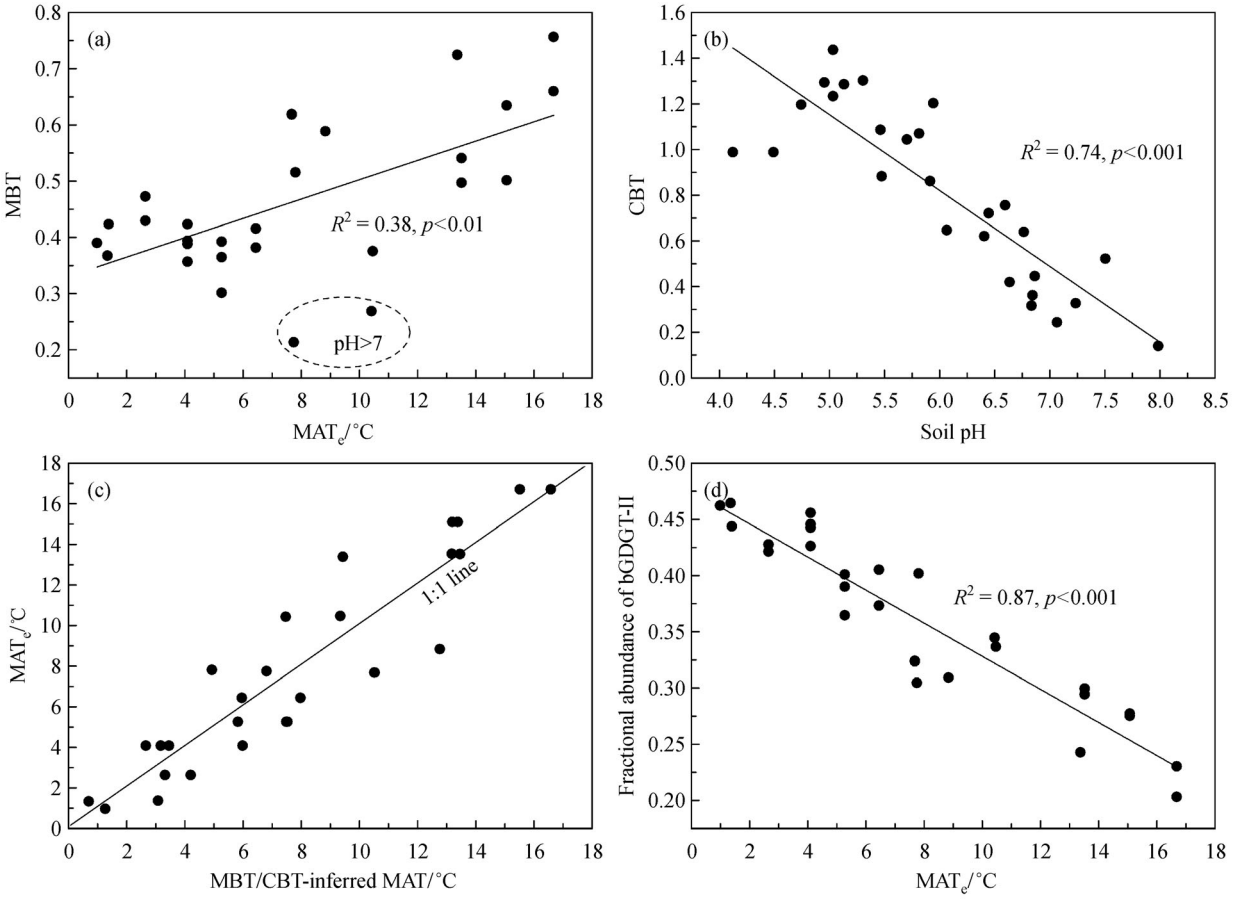

Fig. 5 Cross plots showing the relationship between (a) MBT and MAT_e; (b) CBT and soil pH; (c) MAT_e and MBT/CBT-inferred MAT based on Eq. (8a); (d) fractional abundance of bGDGT-II and MAT_e.

(Fig. 5(b)):

$$\mathrm{CBT} = 2.74 - 0.32 \times \mathrm{pH} \quad (R^2 = 0.74,\ p<0.001), \tag{7}$$

where the constant and coefficient are both less than those for the global and Chinese calibrations (Weijers et al., 2007; Yang et al., 2014). Combining Eq. (6) and Eq. (7), a new local calibration for MBT/CBT and MAT (or altitude) is obtained:

$$\mathrm{MAT} = 2.06 + 28.13 \times \mathrm{MBT} - 9.06 \times \mathrm{CBT} \quad (R^2 = 0.84,\ p<0.001,\ \mathrm{RMSE} = 1.9°\mathrm{C}), \tag{8a}$$

or

$$\mathrm{ALT} = 2704.9 - 4622.3 \times \mathrm{MBT} + 1501.6 \times \mathrm{CBT} \quad (R^2 = 0.84,\ p<0.001,\ \mathrm{RMSE} = 309\,\mathrm{m}), \tag{8b}$$

where ALT and RMSE mean altitude and root mean square error, respectively. This equation more closely resembles the global calibration of Weijers et al. (2007) than the Chinese calibration of Yang et al. (2014) because most soils at Mt. Shennongjia are acidic. However, it has a much lower RMSE than the global calibration of Weijers et al. (2007) (RMSE = 5°C), suggesting that a local calibration can substantially improve the accuracy of absolute temperature and altimetry reconstruction. Besides, MAT has an equivalent dependence on CBT (or pH) and MBT in this equation, which differs from the global and Chinese local calibrations that primarily depend on the MBT index for MAT estimation. The MAT inferred by the MBT/CBT proxy generally tracks the $\mathrm{MAT_e}$ along the 1:1 line (Fig. 5 (c)).

3.4 Complexity of the MBT/CBT being used as a paleoaltimeter

The potential of the MBT/CBT proxy for paleoaltimetry reconstruction has been investigated in a total of 8 mountains worldwide, including Mt. Jianfengling (Yang et al., 2010), Shennongjia, Xiangpi (Liu et al., 2013), Gongga (Peterse et al., 2009), Meghalaya (Ernst et al., 2013), Kilimanjaro (Sinninghe Damsté et al., 2008), Rungwe (Coffinet et al., 2014), and Andean (Anderson et al., 2014), four of which are situated in China. The MBT/CBT proxy appears to be applicable to all of these mountains for paleoaltimetry reconstruction. Because the calibration models were not available for all of these mountains previously, we used the least square multiple regression method with SPSS software for developing the calibration models for the altimetry reconstruction of all eight mountains (Table 3). The resultant calibration equations differ remarkably in the constants, coefficients, determination factors, and RMSE, suggesting that each mountain has its specific local calibration, and none of these can be used universally.

The largest difference among the above equations occurs between regression coefficients for CBT, i.e., Mt. Xiangpi and Andean both yield negative regression coefficients for CBT whereas the others show the opposite trend. These differences likely result from different lapse rates as well as varied environmental impacts on bGDGT distributions. Mt. Xiangpi is the only mountain subjected to a cold and arid climate dominated by alkaline soils. Due to generally high soil pH in semi-arid and arid regions, Yang et al. (2014) developed a different calibration for the reconstruction of paleotemperature for semi-arid and arid regions. The high soil pH in these regions may lead to significantly lower MBT and CBT values than those in humid regions, which in turn results in a large regression coefficient for MBT and a negative coefficient for CBT in the calibration for Mt. Xiangpi. A similar situation might also exist in the humid regions where alkaline and neutral soils could be present due to the weathering of limestone or dolomite. For example, the two soils with pH > 7 (Sample Nos: 8-4 and 10-2) are remarkably different in MBT and CBT values from other acid soils in Mt. Shennongjia; larger errors will be present if the local calibration (Eq. (8b)) is applied to these two alkaline or neutral soils. Therefore, the MBT/CBT as a paleoaltimetry proxy necessitates the development of local calibration. Even so, the occasional

Table 3 Different calibration models for mountains worldwide

Mountain Name	Calibration model	R^2	p value	RMSE/m	Reference
Mt. Kilimanjaro	ALT = 5199.6–5590.3×MBT + 856.6×CBT	0.76	< 0.001	231	Sinninghe Damsté et al. (2008)
Mt. Meghalaya	ALT = 7574.0–9455.6×MBT + 1362.0×CBT	0.70	< 0.001	296	Ernst et al. (2013)
Mt. Jianfengling	ALT = 3346.2–4135.7×MBT + 784.0×CBT	0.55	< 0.05	290	Yang et al. (2010)
Mt. Shennongjia	ALT = 2704.9–4622.3×MBT + 1501.6×CBT	0.84	< 0.001	309	This study
Mt. Gongga	ALT = 2694.7–3338.7×MBT + 1344.4×CBT	0.80	< 0.001	307	Peterse et al. (2009)
Mt. Xiangpi	ALT = 5220.5–10001.9×MBT–819.1×CBT	0.66	< 0.001	87	Liu et al. (2013)
Mt. Rungwe	ALT = 3104.1–4047.2×MBT + 1592.5×CBT	0.82	< 0.001	276	Coffinet et al. (2014)
Mt. Andean	ALT = 5057.5–4347.5×MBT–144.9×CBT	0.63	< 0.001	629	Anderson et al. (2014)

occurrence of alkaline soils in some mountains that feature a dominance of acid soils will bias paleoaltimetry estimation by local calibrations.

Uncertainty in the use of the MBT/CBT proxy as a paleoaltimeter also comes from the underlying mechanism. The MBT proxy, reflecting the methylation degree of bGDGTs, was found to depend primarily on temperature, and to a lesser extent on pH, in both soils and lakes (Weijers et al., 2007; Tierney et al., 2010; Sun et al., 2011; Peterse et al., 2012; Yang et al., 2014). The increase in the methylation degree of bGDGTs was believed to enable bacterial cell membranes to remain in a liquid crystalline state at lower temperatures (Weijers et al., 2007; Peterse et al., 2012; Yang et al., 2014). The MBT/CBT proxy for paleotemperature reconstruction, as classically interpreted, largely relies on the response of MBT to temperature (Weijers et al., 2007). However, in five of the eight mountains, MBT shows weak or no correlation with altitude or temperature (R^2 = 0.03, 0.00, 0.01, 0.38, and 0.39 for Mt. Gongga, Meghalaya, Jianfengling, Shennongjia, and Rungwe, respectively), which throws doubt on the interpretation of the underlying mechanism of the MBT/CBT as a paleoaltimeter in these mountains.

Closer inspection reveals that CBT for Mt. Gongga, Meghalaya, Jianfengling, Rungwe, and Shennongjia exhibited moderate positive correlations with altitude or negative correlations with temperature (R^2 = 0.56, 0.31, 0.43, 0.48, and 0.30, respectively), which cannot be simply explained by the co-variation among CBT, pH, and altitude (or temperature). Because the CBT index essentially reflects the cyclization degree of bGDGTs, precursor bacteria are likely to increase the cyclopentyl rings of bGDGTs in response to higher temperatures in a similar way to the isoprenoid GDGTs of marine Thaumarchaeota (Schouten et al., 2002). In fact, the MBT/CBT-inferred MATs for the former three mountains are primarily related to CBT (R^2= 0.59, 0.68, and 0.79, respectively) rather than to MBT (R^2 = 0.02, 0.04, and 0.02, respectively), suggesting that CBT plays a critical role in temperature or altitude reconstruction for these three mountains. This undoubtedly challenges the classical interpretation of the mechanism of the MBT/CBT proxy and further complicates the use of the MBT/CBT proxy for paleoaltimetry reconstruction. Overall, care should be taken in applying the MBT/CBT proxy to paleoaltimetry reconstruction at a given mountain before the mechanistic control is fully understood.

3.5 Fractional abundance of bGDGTs as paleoaltimetry

A further statistical analysis using RDA reveals that the fractional abundance of bGDGT (%bGDGT) for Mt. Shennongjia has different reliance on MAT_e (or altitude) and soil pH (Fig. 4). Among the acyclic bGDGTs, % bGDGT-II has the highest correlation with MAT_e (R^2 = 0.87, $p < 0.001$), whereas %bGDGT-I and III show no and weak relationships with MAT_e, respectively (R^2 = 0.09 and R^2 = 0.35) (Fig. 4 and Table 4), yielding a calibration equation for the former:

$$\mathrm{MAT} = -59.6 \times f(\mathrm{II}) + 29.24$$
$$(R^2 = 0.87,\ p<0.001,\ \mathrm{RMSE} = 1.7°\mathrm{C}), \quad (9a)$$

or

$$\mathrm{ALT} = 9845 \times f(\mathrm{II}) - 1773$$
$$(R^2 = 0.88,\ p<0.001,\ \mathrm{RMSE} = 275\,\mathrm{m}). \quad (9b)$$

The relationship between %bGDGT and MAT_e at Mt. Shennongjia differs significantly from those for global (Peterse et al., 2012) and Chinese datasets (Yang et al., 2014), where three acyclic bGDGTs (I, II, and III) all exhibited high correlations with MAT. The large variability of %bGDGTs dependence on temperature in these calibrations suggests that bGDGT-producing bacteria may have different responses to temperature, largely depending on the locality. Therefore, in order to identify accurately the constraints of MAT or paleoaltimetry at a given mountain or plateau, local rather than global calibrations are needed.

The MBT index integrates f(I), f(Ib), and f(Ic), and shows poor to moderate correlations with MAT_e at Mt. Shennongjia (R^2 = 0.09, 0.57, and 0.38, respectively; Table 4). Moreover, the %bGDGT-I appears to be more closely related to soil pH (R^2= 0.44, $p < 0.05$) than to MAT_e (R^2 = 0.09). Thus it's reasonable to conclude that MBT is weakly correlated with MAT_e for Shennongjia soils. The stepwise selection method (SSM) by SPSS software can be used to effectively identify the individual %bGDGT that might be sensitive to temperature, and can be used to develop a calibration model that is better than the classically used MBT/CBT proxy (Yang et al., 2014). The different individual %bGDGTs (I, II, III, Ib, and IIb etc.) were gradually added in order to generate different calibration models. An F-test was performed, determining the significance of the addition of each variable, which was then stopped when addition was no longer significant. The final calibration models only include f(II) and f(Ib) as independent variables:

$$\mathrm{MAT} = 23.89 - 49.68 \times f(\mathrm{II}) + 23.07 \times f(\mathrm{Ib})$$
$$(R^2 = 0.88,\ p<0.001,\ \mathrm{RMSE} = 1.5°\mathrm{C}), \quad (10a)$$

or

$$\mathrm{ALT} = -888.4 + 8204.3 \times f(\mathrm{II}) - 3780.4 \times f(\mathrm{Ib})$$
$$(R^2 = 0.89,\ p<0.001,\ \mathrm{RMSE} = 251\,\mathrm{m}). \quad (10b)$$

These equations have higher determination factors but

Table 4 Correlation matrix of fractional abundances of bGDGTs and environmental variables for 28 soils of Mt. Shennongjia

		Altitude	MAT_e	pH	SWC	I	II	III	Ib	Ic	IIb	IIc	IIIb	IIIc
Altitude	*r*	1.00												
	p value													
MAT_e	*r*	**–1.000****	1.00											
	p value	0.00												
pH	*r*	**–0.398***	**0.397***	1.00										
	p value	0.04	0.04											
SWC	*r*	**0.841****	**–0.839****	–0.570**	1.00									
	p value	0.00	0.00	0.00										
I	*r*	–0.30	0.30	**–0.668****	–0.07	1.00								
	p value	0.12	0.12	0.00	0.74									
II	*r*	**0.930****	**–0.928****	–0.34	**0.879****	–0.37	1.00							
	p value	0.00	0.00	0.08	0.00	0.06								
III	*r*	**0.576****	**–0.577****	0.37	0.30	**–0.824****	**0.563****	1.00						
	p value	0.00	0.00	0.06	0.14	0.00	0.00							
Ib	*r*	**–0.742****	**0.741****	**0.555****	**–0.699****	–0.14	**–0.671****	–0.29	1.00					
	p value	0.00	0.00	0.00	0.00	0.48	0.00	0.13						
Ic	*r*	**–0.617****	**0.618****	**0.582****	**–0.598****	–0.16	**–0.530****	–0.31	**0.707****	1.00				
	p value	0.00	0.00	0.00	0.00	0.43	0.00	0.10	0.00					
IIb	*r*	–0.30	0.29	**0.854****	**–0.513****	**–0.758****	–0.29	**0.478***	**0.499****	**0.391***	1.00			
	p value	0.13	0.13	0.00	0.01	0.00	0.14	0.01	0.01	0.04				
IIc	*r*	–0.34	0.34	**0.829****	**–0.468***	**–0.668****	–0.30	0.28	**0.570****	**0.690****	**0.850****	1.00		
	p value	0.07	0.08	0.00	0.02	0.00	0.12	0.15	0.00	0.00	0.00			
IIIb	*r*	–0.22	0.22	**0.688****	**–0.464***	**–0.642****	–0.27	**0.531****	**0.397***	0.10	**0.894****	**0.627****	1.00	
	p value	0.25	0.26	0.00	0.02	0.00	0.16	0.00	0.04	0.60	0.00	0.00		
IIIc	*r*	0.10	–0.10	0.30	–	–0.21	0.00	0.34	–0.07	0.00	0.17	0.22	0.16	1.00
	p value	0.61	0.61	0.12	0.00	0.28	0.99	0.08	0.72	0.98	0.39	0.26	0.41	

Note: ** Correlation is significant at the 0.01 level (two-tailed); * correlation is significant at the 0.05 level (two-tailed); the correlation coefficient (*r*) values with corresponding *p* value < 0.05 are in bold.

lower RMSEs than Eqs. (8a) and (8b), suggesting that they can produce more reliable MAT and paleoaltimetry estimates than the classic MBT/CBT proxy at Mt. Shennongjia. By extension, we propose that the individual %bGDGT can be a better proxy for paleoaltimetry reconstruction than the MBT/CBT proxy; the former is established after the temperature-insensitive bGDGT subsets are removed.

4 Conclusions

The bGDGTs distributions and associated environmental variables for a total of 28 surface soil samples from an altitudinal transect of Mt. Shennongjia in China were investigated in order to determine the potential of bGDGT-based proxies for paleoaltimetry reconstruction. The MBT proxy exhibits only a weak correlation with altitude or MAT estimated based on a previously developed transfer function (MAT_e), which is likely to be explained by a poor relationship between %bGDGT-I and MAT_e. The response of MBT and CBT indices to temperature or pH varies among sites. This necessitates the establishment of local calibrations for paleoaltimetry. The occasional occurrence of alkaline soils in acid soil-dominated regions may produce large errors in paleoaltimetry reconstruction because these alkaline soils may have significantly lower MBT and CBT values than other acid soils. The altitude reconstructed by the MBT/CBT proxy for three mountains largely relies on the CBT index, which apparently contradicts the classical interpretation that depends on MBT. Therefore, caution should be taken in using the MBT/CBT proxy as a paleoaltimeter at a given mountain unless the mechanism for this proxy is fully understood.

The use of an alternative paleothermometer or paleoaltimeter based on the fractional abundance of bGDGTs is suggested as a possible improvement over the MBT/CBT proxy. The accuracy of altitude estimation can potentially

be improved by using this process, in which the bGDGTs subsets showing the most sensitive responses to temperature can be targeted and used to establish the local calibration by a stepwise selection method at a given mountain.

Acknowledgements We would like to thank Yangmin Qin, Xianyu Huang and Canfa Wang for soil sampling and Weihua Ding for LC-MS maintenance. This work was supported by the National Basic Research Program of China (No. 2011CB808800), the National Natural Science Foundation of China (Grant Nos. 41330103 and 41103079) and 111 Project (Grant No. B08030).

References

Anderson V J, Shanahan T M, Saylor J E, Horton B K, Mora A R (2014). Sources of local and regional variability in the MBT'/CBT paleotemperature proxy: insights from a modern elevation transect across the Eastern Cordillera of Colombia. Org Geochem, 69: 42–51

Coffinet S, Huguet A, Williamson D, Fosse C, Derenne S (2014). Potential of GDGTs as a temperature proxy along an altitudinal transect at Mount Rungwe (Tanzania). Org Geochem, 68: 82–89

Dirghangi S S, Pagani M, Hren M T, Tipple B J (2013). Distribution of glycerol dialkyl glycerol tetraethers in soils from two environmental transects in the USA. Org Geochem, 59: 49–60

Ernst N, Peterse F, Breitenbach S F M, Syiemlieh H J, Eglinton T I (2013). Biomarkers record environmental changes along an altitudinal transect in the wettest place on Earth. Org Geochem, 60: 93–99

Ghosh P, Garzione C N, Eiler J M (2006). Rapid uplift of the Altiplano revealed through ^{13}C-^{18}O bonds in paleosol carbonates. Science, 311 (5760): 511–515

Hren M T, Pagani M, Erwin D M, Brandon M (2010). Biomarker reconstruction of the early Eocene paleotopography and paleoclimate of the northern Sierra Nevada. Geology, 38(1): 7–10

Huguet C, Hopmans E C, Febo-Ayala W, Thompson D H, Sinninghe Damsté J S, Schouten S (2006). An improved method to determine the absolute abundance of glycerol dibiphytanyl glycerol tetraether lipids. Org Geochem, 37(9): 1036–1041

Jia G, Wei K, Chen F, Peng P A (2008). Soil *n*-alkane δD vs. altitude gradients along Mount Gongga, China. Geochim Cosmochim Acta, 72(21): 5165–5174

Liu W, Wang H, Zhang C L, Liu Z, He Y (2013). Distribution of glycerol dialkyl glycerol tetraether lipids along an altitudinal transect on Mt. Xiangpi, NE Qinghai-Tibetan Plateau, China. Org Geochem, 57: 76–83

Loomis S E, Russell J M, Sinninghe Damsté J S (2011). Distributions of branched GDGTs in soils and lake sediments from western Uganda: implications for a lacustrine paleothermometer. Org Geochem, 42(7): 739–751

Luo P, Peng P A, Gleixner G, Zheng Z, Pang Z, Ding Z (2011). Empirical relationship between leaf wax *n*-alkane δD and altitude in the Wuyi, Shennongjia and Tianshan Mountains, China: implications for paleoaltimetry. Earth Planet Sci Lett, 301(1–2): 285–296

Mulch A, Graham S A, Chamberlain C P (2006). Hydrogen isotopes in Eocene river gravels and paleoelevation of the Sierra Nevada. Science, 313(5783): 87–89

Mulch A, Teyssier C, Cosca M A, Vanderhaeghe O, Vennemann T W (2004). Reconstructing paleoelevation in eroded orogens. Geology, 32(6): 525–528

Peterse F, van der Meer J, Schouten S, Weijers J W H, Fierer N, Jackson R B, Kim J H, Sinninghe Damsté J S (2012). Revised calibration of the MBT – CBT paleotemperature proxy based on branched tetraether membrane lipids in surface soils. Geochim Cosmochim Acta, 96: 215–229

Peterse F, van der Meer M T J, Schouten S, Jia G, Ossebaar J, Blokker J, Sinninghe Damsté J S (2009). Assessment of soil *n*-alkane δD and branched tetraether membrane lipid distributions as tools for paleoelevation reconstruction. Biogeosciences, 6(12): 2799–2807

Polissar P J, Freeman K H, Rowley D B, McInerney F A, Currie B S (2009). Paleoaltimetry of the Tibetan Plateau from D/H ratios of lipid biomarkers. Earth Planet Sci Lett, 287(1–2): 64–76

Rowley D B, Garzione C N (2007). Stable isotope-based paleoaltimetry. Annu Rev Earth Planet Sci, 35(1): 463–508

Ruddiman W F, Kutzbach J E (1989). Forcing of late Cenozoic northern hemisphere climate by plateau uplift in southern Asia and the American west. J Geophys Res Atmos, 94(D15): 18409–18427

Schouten S, Hopmans E C, Schefuß E, Sinninghe Damsté J S (2002). Distributional variations in marine crenarchaeotal membrane lipids: a new tool for reconstructing ancient sea water temperatures? Earth Planet Sci Lett, 204(1–2): 265–274

Sinninghe Damsté J S, Hopmans E, Pancost R D, Schouten S, Geenevasen J A J (2000). Newly discovered non-isoprenoid glycerol dialkyl glycerol tetraether lipids in sediments. Chem Commun (Camb), 2000(17): 1683–1684

Sinninghe Damsté J S, Ossebaar J, Schouten S, Verschuren D (2008). Altitudinal shifts in the branched tetraether lipid distribution in soil from Mt. Kilimanjaro (Tanzania): implications for the MBT/CBT continental palaeothermometer. Org Geochem, 39(8): 1072–1076

Sun Q, Chu G, Liu M, Xie M, Li S, Ling Y, Wang X, Shi L, Jia G, Lu H Y (2011). Distributions and temperature dependence of branched glycerol dialkyl glycerol tetraethers in recent lacustrine sediments from China and Nepal. J Geophys Res, 116(G1): G01008

ter Braak C J F (1988). Canoco-a FORTRAN program for canonical community ordination by (partial) (detrended) (canonical) correspondence analysis, principal components analysis and redundancy analysis (version 2.1). Technical Rep. LWA-88-02, GLW, Wageningen, 95

ter Braak C J F, Prentice I C (1988). A theory of gradient analysis. Adv Ecol Res, 18: 271–317

ter Braak C J F, Smilauer P (2002). CANOCO reference manual and Canodraw for Windows Users Guide: software for canonical community ordination (version 4.5). Microcomputer Power, Ithaca, NY, USA. 500

Tierney J E, Russell J M, Eggermont H, Hopmans E C, Verschuren D, Sinninghe Damsté J S (2010). Environmental controls on branched tetraether lipid distributions in tropical East African lake sediments. Geochim Cosmochim Acta, 74(17): 4902–4918

Weijers J W H, Schouten S, Spaargaren O C, Sinninghe Damsté J S (2006). Occurrence and distribution of tetraether membrane lipids in soils: implications for the use of the TEX_{86} proxy and the BIT index. Org Geochem, 37(12): 1680–1693

Weijers J W H, Schouten S, van den Donker J C, Hopmans E C, Sinninghe Damsté J S (2007). Environmental controls on bacterial tetraether membrane lipid distribution in soils. Geochim Cosmochim Acta, 71(3): 703–713

Weijers J W H, Steinmann P, Hopmans E C, Schouten S, Sinninghe Damsté J S (2011). Bacterial tetraether membrane lipids in peat and coal: testing the MBT/CBT temperature proxy for climate reconstruction. Org Geochem, 42(5): 477–486

Weijers J W H, Wiesenberg G L B, Bol R, Hopmans E C, Pancost R D (2010). Carbon isotopic composition of branched tetraether membrane lipids in soils suggest a rapid turnover and a heterotrophic life style of their source organism(s). Biogeosciences, 7(9): 2959–2973

Yang H, Ding W, He G, Xie S (2010). Archaeal and bacterial tetraether membrane lipids in soils of varied altitudes in Mt. Jianfengling in South China. J Earth Sci, 21(S1): 277–280

Yang H, Ding W, Wang J, Jin C, He G, Qin Y, Xie S (2012). Soil pH impact on microbial tetraether lipids and terrestrial input index (BIT) in China. Science China Earth Sciences, 55(2): 236–245

Yang H, Ding W, Zhang C L, Wu X, Ma X, He G, Huang J, Xie S (2011). Occurrence of tetraether lipids in stalagmites: implications for sources and GDGT-based proxies. Org Geochem, 42(1): 108–115

Yang H, Pancost R D, Dang X, Zhou X, Evershed R P, Xiao G, Tang C, Gao L, Guo Z, Xie S (2014). Correlations between microbial tetraether lipids and environmental variables in Chinese soils: optimizing the paleo-reconstructions in semi-arid and arid regions. Geochim Cosmochim Acta, 126: 49–69

Zhu C, Chen X, Zhang G, Ma C, Zhu Q, Li Z, Xu W (2008). Spore-pollen-climate factor transfer function and paleoenvironment reconstruction in Dajiuhu, Shennongjia, Central China. Chin Sci Bull, 53 (S1): 42–49